



An activated fluid stream – New techniques for cold water cleaning

Peter R. Birkin^{a,*}, Douglas G. Offin^a, Timothy G. Leighton^b



^a Chemistry, Natural and Environmental Sciences, University of Southampton, Southampton SO17 1BJ, UK

^b Institute of Sound and Vibration Research, Engineering and the Environment, University of Southampton, Southampton SO17 1BJ, UK

ARTICLE INFO

Article history:

Received 4 November 2014

Received in revised form 27 August 2015

Accepted 1 October 2015

Available online 9 October 2015

Keywords:

Bubble swarm

Cleaning

Stream

Ultrasound

Electrochemical

ABSTRACT

Electrochemical, acoustic and imaging techniques are used to characterise surface cleaning with particular emphasis on the understanding of the key phenomena relevant to surface cleaning. A range of novel techniques designed to enhance and monitor the effective cleaning of a solid/liquid interface is presented. Among the techniques presented, mass transfer of material to a sensor embedded in a surface is demonstrated to be useful in the further exploration of ultrasonic cleaning of high aspect ratio micropores. In addition the effect of micropore size on the cleaning efficacy is demonstrated. The design and performance of a new cleaning system reliant on the activation of bubbles within a free flowing stream is presented. This device utilised acoustic activation of bubbles within the stream and at a variety of substrates. Finally, a controlled bubble swarm is generated in the stream using electrolysis, and its effect on both acoustic output and cleaning performance are compared to the case when no bubbles are added. This will demonstrate the active role that the electrochemically generated bubble swarm can have in extending the spatial zone over which cleaning is achieved.

© 2015 Elsevier B.V. All rights reserved.

1. Introduction

The cleaning of a material or an interface is at the centre of many processes which are important to health or to the production of high value commodities. This cleaning process should be fast, efficient (in terms of consumables and energy) and cause the least possible damage to the substrate while removing the target contaminate from the surface in question. While there are undoubtedly many possible methods to achieve these goals, in a variety of processes ultrasonic cleaning of an interface has been found to be useful [1–3]. In this technology the interaction of sound with materials and bubbles (which generates unusual physical and chemical conditions [4–8] within a fluid) has led to a rich set of exploited technologies and fascinating technical challenges. At the heart of ultrasonic cleaning is the interaction between sound and gas bubbles [9,10]. However, this interaction is complex [11] and the environments within which they occur can have intricate geometries [12]. Amongst the technological approaches used, the cleaning bath is perhaps the most well-known although other systems (for example ‘megasonic fields’ which have been explored with electrochemical probes [13,14]) are noteworthy. While the immersion of an object in a cleaning bath is undoubtedly effective in many examples, this approach has limitations [15]. For example

the presence of areas of the bath which are active (so called ‘hot spots’) and areas which are inactive (‘cold spots’) could result in uneven treatment of a sample [16]. In order to characterise this spatial variation, cleaning activity can be mapped through the use of electrochemical [17–20], imaging [21–23] and acoustic measurements [24,25]. In addition local activity has also been correlated with cell death [26]. However, the location of cavitation hot spots will also depend on the immersion of an object into the bath which will also perturb the system [15,27]. Further restrictions are encountered through the spatial requirement for immersion of the sample within the bath. Clearly these limitations are associated with the ‘bath’ itself and could be avoided if this immersion approach was not employed. For example a liquid stream directed at the surface to be cleaned could be envisaged [15,28]. Here the cleaning action of bubbles excited with a suitable ultrasonic field should be generated at the end of a fluid stream. In addition low flow rates of fluid within this approach are useful in releasing the contaminant from the surface and avoiding re-deposition at another location (a further possible limitation in bath geometries). The low velocity stream approach has many advantages; however, two basic criteria are necessary for this strategy to be successful. First, the sound field must be sufficient to generate bubble activity at the solid/liquid interface of the material to be cleaned. Second, a suitable bubble population must also be present. This population can then be driven by the sound field deployed and act on the contaminant at the interface in question (through suitable oscillation

* Corresponding author.

E-mail address: prb2@soton.ac.uk (P.R. Birkin).

[29–31] and shear forces [32] for example [30,31]). These two requirements are by no means trivial to create within a flowing stream [33,34]. However, such an approach has been adopted in an ultrasonically activated stream (UAS). In this case the device, which has been constructed to fulfil the requirements outlined above, can operate in an aqueous environment under ambient conditions without the need to add chemical additives to the media. While this simple approach has many advantages, there may be other circumstances when the naturally occurring bubble population is limiting. Under these circumstances an approach with an introduced appropriate bubble population (or bubble swarms) may aid the cleaning of an interface. One strategy for the generation of such conditions is the use of electrochemically generated bubble swarms. This approach is highlighted here, with the effect of the bubble population on the pressure field within the fluid stream and the cleaning of a fluorescent material from a large surface area structure reported.

2. Experimental

Micropores and large extended surfaces were chosen in this study for a number of reasons. First, micropores represent an occluded geometry where conventional fluid flow is particularly ineffective. In this environment the ability of acoustically excited gas bubbles is highlighted through the rapid decontamination of the pore in question. Second, the pore is well suited for the employment of electrochemical sensing approaches which enable some degree of quantification of the process. Third, the appropriate use of transparent media for the micropore electrode substrate allows for high-speed visualisation to be performed simultaneously with the electrochemical experiments in efforts to investigate the mechanistic details of the cleaning process. Lastly, extended surfaces (e.g. the fluorescent loaded tiles) are also pertinent as they illustrate the effect of the bubble population on surface cleaning over a large spatial domain.

Micropores were generated using an electrochemical etching approach [35]. Micropore experiments were performed as reported elsewhere [12] using a 23 kHz piston like emitter (or ultrasonic horn) immersed in an electrochemical cell and set 5 mm away from the surface of the electrode body containing the micropore. In these experiments a 0.1 M $\text{Sr}(\text{NO}_3)_2$ (Sigma-Aldrich, 99+%), 5 mM $\text{K}_3[\text{Fe}(\text{CN})_6]$ (Alfa Aesar, 99.97%) and F54 (dstl) emulsion was used. The contaminant was a polymer thickened methyl salicylate matrix (dstl).

A brief experimental protocol and description of the construction and operation of the electrochemically enhanced UAS (or e^2 UAS) device is given here. The device is based on a rho-c matched cone or horn (matched to the acoustic impedance of water) attached to an ultrasonic transducer. Complete UAS devices (or StarStream systems) can be obtained from Ultrawave Ltd (F0030001). Note, the UAS concept (including the use of electrochemically generated bubbles swarms to enhance cleaning) was detailed in 2011 [28].

Bubble swarms, generated through controlled electrolysis within the UAS structure, were produced from 100 μm diameter Pt microwires (Advent research Materials) inserted so that they bisected the flow of liquid. These wires were used to electrolyse water by applying 24 Vdc for a variety of time periods (5–30 ms) in a controlled manner with respect to the sound field (which was also operated in a pulsed mode). The timing control of both the sound field and the electrochemical bubble swarm was achieved using a microprocessor interfaced to a PC through a RS232 connection and software written in-house (Visual Basic 6). The ultrasonic signal was generated by a gated (by the microprocessor) TTI2512a function generator (530 mV peak-to-peak amplitude) and an E&I power amp (240L). The solution consisted

of 0.1 M Na_2SO_4 (Fisher lab reagent) and 2 mM sodium dodecyl sulphate (Sigma 98%+) prepared under aerobic conditions. In the UAS experiments reported here a closed loop flow system was used where 1.5 dm^3 of the electrolyte media was pumped (up to 3 $\text{dm}^3 \text{min}^{-1}$) around the system using a small pump (Totton pumps NDP 14/2). Pressure measurements were made using a pressure sensor calibrated to a Bruel & Kjaer 8103 hydrophone in the frequency range used placed ~ 1 cm from the nozzle of the horn/cone structure of the UAS device. The data was recorded using a Handyscope HS3 (Tiepie Engineering) USB oscilloscope using an average of 32 pulses in each case. Images of the fluorescent particulate tracer (Wash & Glow UV Germ Fluid, Glowtec) were taken in the dark and illuminated with a UV lamp. Domestic ceramic tiles (~ 10 cm square, 5 mm thick) were used to assess the spatial extent of cleaning using the activated stream technology. These ceramic tiles were loaded with several (~ 3) drops, spread by a gloved hand and allowed to dry for 15 min before use. Each tile was treated with a UAS or e^2 UAS for a period of 10–15 s. All chemicals were used as supplied.

3. Results and discussion

While many protocols and systems have been deployed to investigate the cleaning ability of ultrasonic fields, electrochemical technology has a number of major advantages [17,32,36,37,14]. Electrodes may be embedded into the substrate in question and in turn recessed to achieve a more complex representative substrate onto which cleaning experiments can be performed. Such an approach has been used to demonstrate the ability of ultrasound to remove an electrochemically inert matrix from a micropore structure [12]. Offin et al. showed that bulk fluid flow was ineffective in comparison to bubble activity captured in the micropore. Here we extend this approach and explore surface cleaning in an immersed electrode/sound source arrangement. However, the dimensions of the micropores deployed are further reduced while increasing the recess depth employed. This has the effect of increasing the aspect ratio of the pore and hence enables the exploration of the ability of activated gas bubbles to remove material from these structures. Fig. 1(a) and (b) shows two schematic representations of the micropore and acoustically excited bubbles that result in pore cleaning. Note that bubbles, which in the absence of a suitable sound field are inactive, can if excited have oscillating ripples (Faraday waves) induced on their surfaces and this has been shown to generate local shear [31,32] and convection (microstreaming) [38–40]. Such acoustically excited bubbles enter the outer layers of the inert liquid and start to remove material [12]. Fig. 1(a) shows a representation of a micropore filled with an electrochemically inert matrix (here tMS, coloured in blue in Fig. 1, ■). In this case the electrochemically active molecule present in the bulk (here 'A' or $[\text{Fe}(\text{CN})_6]^{3-}$) of the fluid is unable to reach the electrode surface. Under these conditions, even though the electrode was held under mass transfer limiting conditions for the redox probe employed, the electrode is unable to reduce compound 'A' and no current will be observed ($i=0$). However, the presence of oscillating gas bubbles, driven by the acoustic field employed, results in penetration of the outer tMS layer and removal of material (as indicated by the arrows) from the micropore. This has been confirmed by high-speed imaging of micropore structures in combination to the electrochemical measurements [12]. Fig. 1(b) shows a schematic representation of the pore after the active gas bubbles have removed the inert tMS from the pore. Under these circumstances the electrode is now able to electrochemically reduce compound 'A' to 'A $^-$ ' under mass transfer limiting conditions. Hence an electrochemical current will only be observed as the tMS is removed from the system allowing

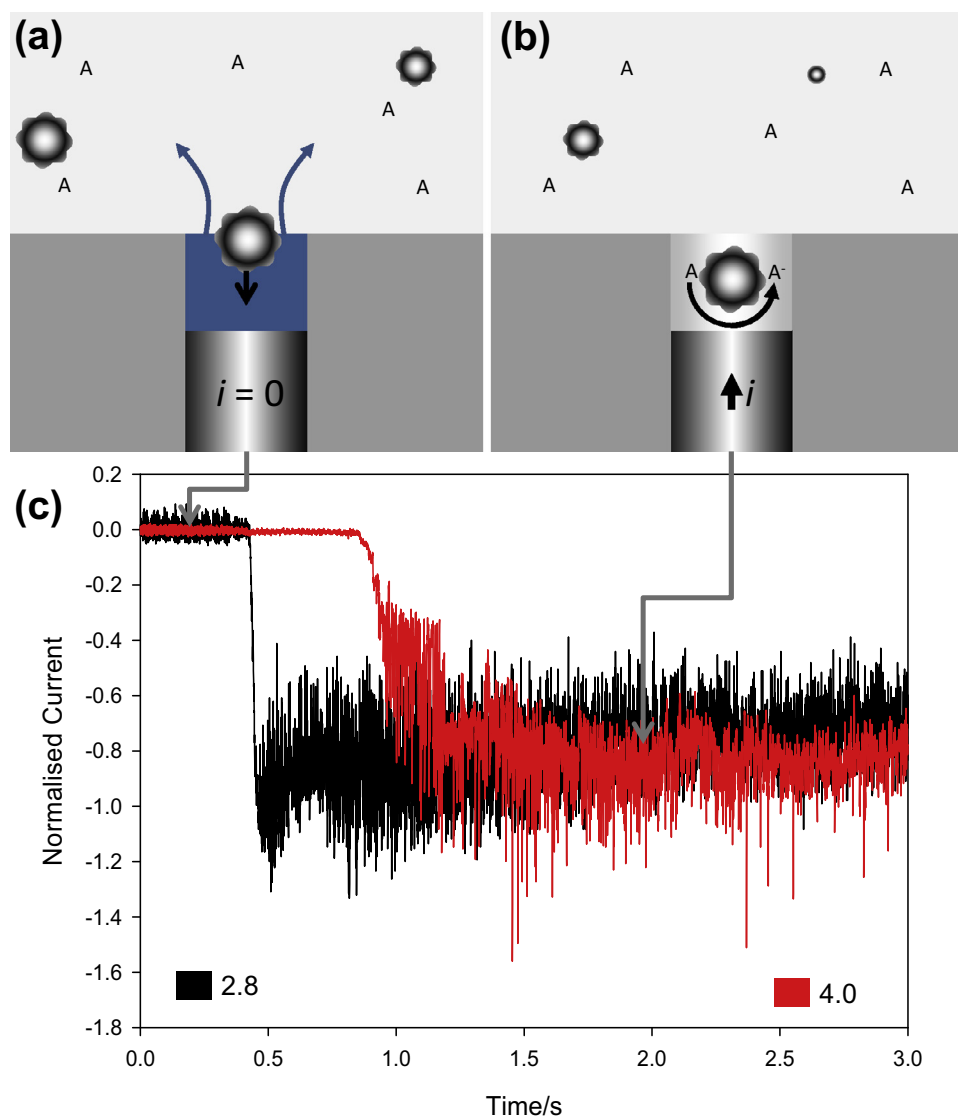


Fig. 1. (a) Schematic showing a recessed electrode filled with an electrochemically inert liquid (■ here tMS). The electrochemically active redox probe (A) in the bulk of the media is unable to get the electrode surface and no current flows. (b) Schematic showing the recessed electrode after bubble mediated cleaning of the recess is complete. Now electrochemical reduction of 'A' to 'A⁻' occurs at the solid/liquid interface of the Pt electrode and a current is detected. Both (a) and (b) are linked to the current time histories by the arrows to indicate the electrochemical signal detected by the electrode at that point in the experiment. (c) Plot showing the current normalised to the current recorded for a clean electrode (note here shown as a negative to indicate the cathodic nature of the process) measured as a function of time for contaminated recessed Pt electrodes exposed to ultrasound from a piston like emitter at an electrode to source distance of 5 mm. Note the sound source was initiated at $t = 0$ s. In the case of the black line (—) the aspect ratio of the cavity was 2.8 (electrode diameter 125 μm) and in the case of the red line (—) it was 4.0 (electrode diameter 50 μm). In both cases the current has been normalised to the average current recorded for corresponding clean electrodes under identical bulk solution conditions. The aerobic solution contained F54 emulsion with 5 mM $\text{K}_3\text{Fe}(\text{CN})_6$ and 0.1 M $\text{Sr}(\text{NO}_3)_2$. The potential of the electrode was held at 0 V vs. SCE. The experiment was performed under ambient conditions (20–25 °C). (For interpretation of the references to colour in this figure legend, the reader is referred to the web version of this article.)

compound 'A' to reach the electrode (here Pt) at the base of the pore. This approach has been extended here to explore the effect of aspect ratio on the rate at which a pore was cleaned. Fig. 1(c) shows a comparison of a micropore with an aspect ratio of 2.8 to a micropore with an aspect ratio of 4 (note electrode diameter of 125 μm and 50 μm respectively). Fig. 1(c) shows that the pores are cleaned relatively quickly (<1.5 s) but that the smaller pore with the smaller aspect ratio was cleaned in a greater time (~ 1 s (—) compared to ~ 0.4 s (—) for the larger micropore). This data suggested that the cleaning ability of ultrasonically activated gas bubbles is significant and many orders of magnitude faster than that reported for flow generated by an impinging jet (see Ref. [12]) on similar micropore substrates. In addition, the larger the aspect ratio employed the slower the cleaning appears to be. While these experiments are illustrative, they were performed with a

micropore electrode immersed in an electrochemical cell at a defined distance from a piston like emitter source. Clearly in order to create a more versatile cleaning system an ultrasonically activated stream (or UAS) would be more desirable. Here the cleaning action would be created at the end of a low velocity stream. In addition, in the following experiments an electrochemically enhanced UAS ($e^2\text{UAS}$) approach will be adopted. Here, as well as producing significant acoustic fields (through the device design [33,34] and materials used), a bubble swarm [28] will be electrochemically generated in the system and the cleaning ability investigated on a particular fluorescent marker material.

Fig. 2 shows the approach adopted with particular reference to the timing of the electrochemical and acoustic stimuli applied to the system. Note this was found to be a useful approach as continuous electrochemical generation caused significant perturbation in

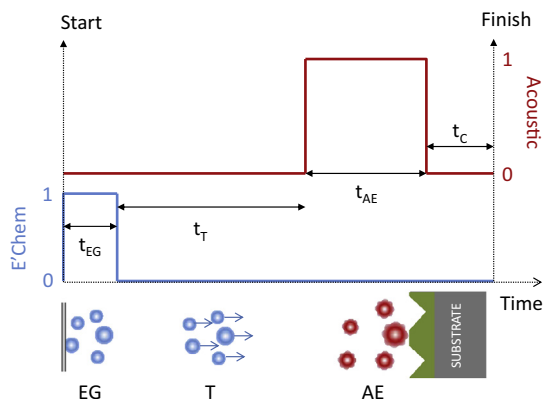


Fig. 2. Schematic showing the pulse sequence used in the cleaning experiments with the e^2 UAS system. Here the blue line (—) shows the activation of the electrochemical bubbles generator for period t_{EG} , while the red line (—) indicates the acoustic excitation of the system for a period t_{AE} . The travel time t_T is also indicated. A short communications time t_C is also indicated, typically 20 ms. This complete sequence is then repeated. The lower panel shows the electrochemical generation at electrodes (EG) and travel T (—) under silent conditions followed by acoustic excitation (—) of the bubble swarm on an appropriate substrate. (For interpretation of the references to colour in this figure legend, the reader is referred to the web version of this article.)

the transmission of the acoustic signal down the stream of fluid to the substrate under investigation. In order to avoid this attenuation of the acoustic signal by the bubble swarm a pulsed approach was adopted. In addition as the electrochemical generation of the bubble swarm and the translation time were performed in the absence of acoustic stimuli, rectified diffusion [41,42] and acoustically driven coalescence will be minimised. In this approach the generation of a dense bubble cloud was achieved through the application of a short burst of potential across two Pt microwire electrodes inserted into the UAS device followed by a delay time to allow the bubble swarm that was generated to be swept to the substrate placed downstream in the liquid flow path. When the bubbles reach the substrate the sound field was initiated for a set period of time to allow cleaning action to be accomplished. The size distribution and number of bubbles generated in the swarm will be dependent on a number of factors including the electrode design, solution conditions and current [28,43]. High-speed imaging of the e^2 UAS system also suggests that a significant bubble density (compared to the solution alone) is present within the swarm [43]. Finally a brief communications period (to allow the electrochemical current passed during the bubble generation phase of the sequence) was added at the end before the complete sequence was repeated. Typically the electrochemical generation period was 10 ms, the transit time was 35 ms (which matched the transit time expected for the flow rate employed and the dimensions of the system) and the acoustic excitation period was 100 ms. A schematic of the various stages in this sequence is shown in the lower panel of Fig. 2.

Fig. 3 shows the effect of the bubble swarm on the pressure detected by a pressure sensor placed 1 cm from the nozzle of the UAS system. Here the pressure time history detected in the absence (—) and presence (—) of a 5 ms (t_{EG}) electrochemical bubble swarm is shown. In the absence of the electrochemical bubble swarm, the pressure field builds to a zero-to-peak amplitude of ~ 250 kPa over a period of ~ 60 ms. In the presence of the bubble swarm the pressure time history clearly shows the presence of the bubble swarm over the surface of the pressure sensor. The bubble swarm reduced the initial pressure field detected by the hydrophone and appears to reduce the overall field during the complete 100 ms time window employed. Fig. 4 shows the

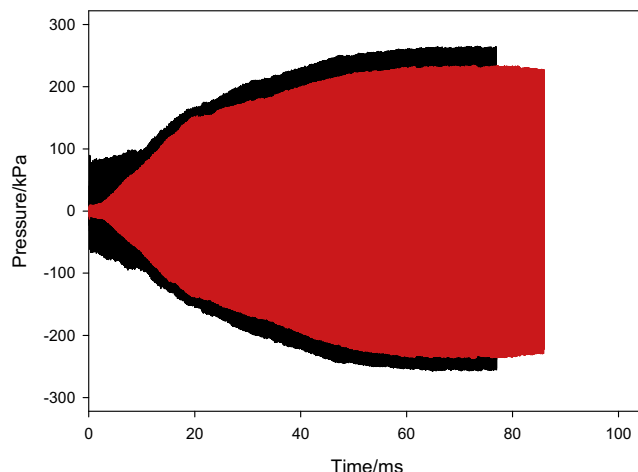


Fig. 3. Plot showing the pressure time histories produced by the e^2 UAS device set 1 cm from a pressure sensor. The values of t_{EG} are 0 and 5 ms for — and — respectively. The values of t_T and t_{AE} are 35 and 100 ms respectively. The solution flow rate was $3 \text{ dm}^3 \text{ min}^{-1}$. The aerobic aqueous solution contained 0.1 M Na_2SO_4 and 2 mM SDS. The solution temperature was 26–28 °C. The ultrasonic frequency was 135.7 kHz.

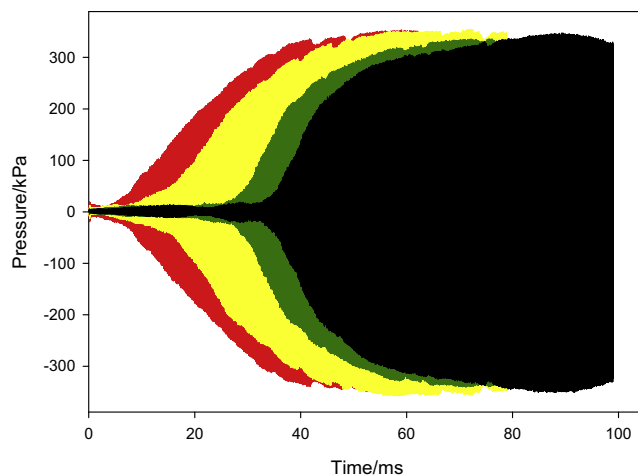


Fig. 4. Plot showing the pressure time histories produced by the e^2 UAS device set 1 cm from a pressure sensor. The values of t_{EG} are 5, 10, 20 and 30 ms for —, —, — and — respectively. The values of t_T and t_{AE} were 35 and 100 ms respectively in all cases. The solution flow rate was $3 \text{ dm}^3 \text{ min}^{-1}$. The aerobic aqueous solution contained 0.1 M Na_2SO_4 and 2 mM SDS. The solution temperature was 26–28 °C. The ultrasonic frequency was 134.8 kHz.

extent of this initial pressure field perturbation as a function of the duration of the electrochemical generation period applied to the swarm generation (see Fig. 2, t_{EG}). In this case the transit time of the swarm to the interface and the ultrasonic activation period remain fixed. Fig. 4 shows that as the length of the electrochemical bubble generation period (t_{EG}) was increased, the extent of the pressure perturbation (or shielding of the hydrophone employed) was increased. For example, the pressure field reaches its maximum value after ~ 50 ms for a 5 ms t_{EG} value while for $t_{EG} = 30$ ms, the pressure field required ~ 80 ms to reach its maximum value. This reflects the longer period of the electrochemical bubble swarm generation and the longer time period required for the bubble swarm to be swept past the acoustic sensor employed. In all cases the pressure field reached essentially the same value at the end of the ultrasonic activation period indicating that once the bubble swarm has past, its effects are minimal (apart from

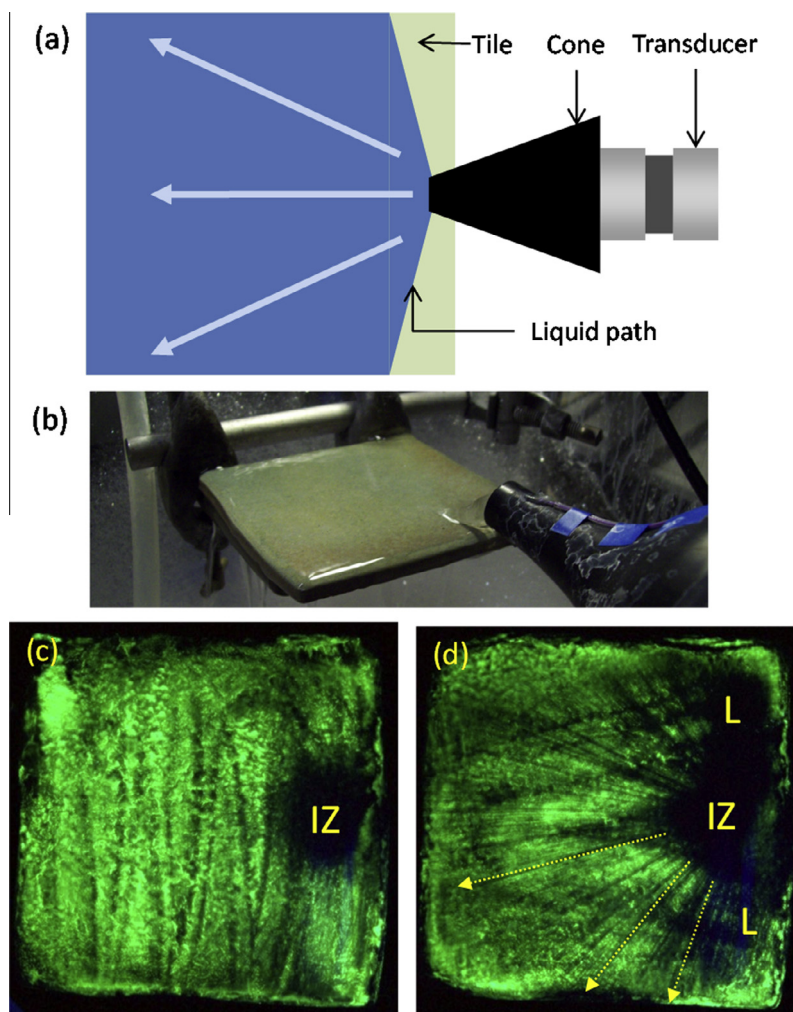


Fig. 5. (a) Schematic showing a top view of the impingement of the e^2 UAS nozzle on a square ceramic tile ($10\text{ cm} \times 10\text{ cm}$) coated with a green fluorescent marker. The coated tile (■) is arranged so that the fluid (■) runs over almost the complete surface. (b) Image showing the experimental arrangement (taken from ~behind the UAS device) showing the stream impinging on the surface (towards the corner of the tile in this case) of the horizontal tile. (c) Image showing a coated tile post treated with the e^2 UAS without the electrochemical generation of the bubble swarm. 'IZ' shows the impingement zone where the inherent bubble population excited by the acoustic field employed removed the fluorescent marker. (d) Image showing a coated tile post treated with the e^2 UAS with the electrochemical generation of the bubble swarm. 'IZ' shows the impingement zone where the bubble population excited by the acoustic field employed removed the fluorescent marker. 'L' indicates side lobes where extra marker has been removed close to the impingement zone. In addition 'streaking' along the complete tile surface is highlighted (just across the lower half of the tile for clarity) where extra 'tracks' of material has been removed by the electrochemically generated bubble swarms as they pass over the complete tile. The solution flow rate was $\sim 2\text{--}2.5\text{ dm}^3\text{ min}^{-1}$. The aerobic aqueous solution contained $0.1\text{ M Na}_2\text{SO}_4$ and 2 mM SDS . The solution temperature was $20\text{--}25\text{ }^\circ\text{C}$. The ultrasonic frequency was $\sim 135\text{ kHz}$. (For interpretation of the references to colour in this figure legend, the reader is referred to the web version of this article.)

the minor reduction in the maximum value reported in Fig. 3). While these results show the effect of the electrochemically generated bubble swarm on the acoustic field detected by the surface under impingement by the stream, they do not demonstrate that this bubble swarm has any marked effect on surface cleaning. This will now be investigated.

Fig. 5 shows an experiment where the spatial extent of surface cleaning generated with the UAS device was investigated using a fluorescent material as a marker for surface cleaning. Here this marker was spread over a horizontal $10 \times 10\text{ cm}$ ceramic tile and the UAS device directed at the edge of the tile so that the stream impinged in one location but the stream was also able to spread across the tile's surface. Fig. 5(a) and (b) shows a schematic (as viewed from above) of this arrangement and an image of the experimental setup respectively. Fig. 5(c) and (d) shows the effect of UAS and e^2 UAS operation respectively on the removal of the fluorescent marker from the tile surface. Fig. 5(c) shows that the UAS device is particularly effective at removing the marker material in the impingement zone (labelled 'IZ' on Fig. 5(c)) which under these

conditions appears as a circular area of radius $\sim 1\text{ cm}$. The rest of the tile does not appear to be affected. Fig. 5(d) shows that the cleaning action delivered by the e^2 UAS system was significantly enhanced with many more features apparent. For example the impingement zone (IZ) is extended with lateral cleaning lobes (denoted by 'L' on Fig. 5(d)) apparent. These lobes (showing additional cleaning action) extend by up to $\sim 4\text{ cm}$ from the fluid streams impingement point. In addition these lobes may also contain further structure/banding. Finally radial streaking is seen to spread across almost the entire surface of the tile (highlighted by the dotted arrows in the lower half of Fig. 5(d)). Clearly, the e^2 UAS system has extended the cleaning action of this approach by a significant amount and it is interesting to speculate that the electrochemically generated bubble swarms remain 'active' as they move across the surface of the tile. These active bubbles (driven by the acoustic field present in all these areas over the tile's surface) presumably oscillate within the sound field present and continue to remove the fluorescent particulate material from the surface of the tile resulting in the additional cleaning seen in these side

lobes and the streaking observed across a significant portion of the tiles surface. However, further experimental evidence is required before strong conclusions can be drawn with respect to the complete picture of the dynamics of the bubbles within this system and over the surface of the substrate. Evidence related to the pressure field in this particular thin film liquid system would also be useful. However, this is by no means trivial considering the geometry of the system employed. It should also be noted that although electrochemical investigations of bubble dynamics in acoustic fields are very useful, some care in the interpretation of the data is necessary. For example mass transfer studies in cavitation environments provides a myriad of electrochemical data [36,44–46]. However, as there are many possible contributions (for example bubbles motion, microstreaming, inertial collapse and acoustic streaming) to the current time response of the electrode (or micro-electrode), attributing a particular current time transient to a specific mechanism is by no means trivial. Further complementary experimental data or control is necessary (for example by limiting the mechanisms present or by employing multiple electrodes [36,40,45] or by combining techniques including high-speed imaging, acoustic characterisation and luminescence imaging etc. [11]) in order for detailed mechanistic information to be gathered. Further discussion of these issues can be found elsewhere [47].

While the cleaning effects are significant, and will undoubtedly be useful in some circumstances, some limitations of the e^2 UAS system should be noted. In the current device, the electrochemical generation of the bubble swarm requires the presence of an electrolyte. This may be limiting under some circumstances but could be avoided with alternative electrochemical generator architectures. In addition the pulsed approach will reduce the exposure of the sample to the acoustic field in comparison to the case where a continuous field is deployed. This could increase the treatment time for a sample, but, as shown here, the additional spatial cleaning range of the e^2 UAS device may outweigh this possible limitation.

Note that these limitations are not encountered for a UAS system. Here efficient cleaning (using water without additives) of a variety of materials (for example surgical steel and bone) has been demonstrated for several different systems (including biofilms, proteins and tissue) [48,49].

4. Conclusions

The e^2 UAS device has been shown to generate significant zero-to-peak pressure amplitudes (>300 kPa zero-to-peak amplitude) under the conditions employed. In addition the bubble swarms generated in the e^2 UAS device shield the pressure developed on the surface of the substrates deployed particularly in the initial stage of the initiation of the ultrasonic field when the swarms attenuate the acoustic signal reaching the sensor. In addition, activated gas bubbles (in an immersed source/electrode arrangement) are able to clean structures with relatively high aspect ratios. Finally acoustically driven bubble swarms, generated electrochemically and excited in a pulsed manner, are also able to extend the spatial range of surface cleaning using the e^2 UAS device.

Acknowledgement

This work was supported by dstl, the 2011 Royal Society Brian Mercer Award for Innovation and Ultrawave Ltd. for which the authors are extremely grateful.

Data supporting this study are openly available from the University of Southampton repository <http://dx.doi.org/10.5258/SOTON/382942>.

References

- [1] S.I. Nikitenko, L. Venault, R. Pflieger, T. Chave, I. Bisel, P. Moisy, Potential applications of sonochemistry in spent nuclear fuel reprocessing: a short review, *Ultrason. Sonochem.* 17 (2010) 1033–1040, <http://dx.doi.org/10.1016/j.ultsonch.2009.11.012>.
- [2] I.J. Seymour, D. Burfoot, R.L. Smith, L.A. Cox, A. Lockwood, Ultrasound decontamination of minimally processed fruits and vegetables, *Int. J. Food Sci. Technol.* 37 (2002) 547–557, <http://dx.doi.org/10.1046/j.1365-2621.2002.00613.x>.
- [3] A. Kumar, R.B. Bhatt, P.G. Behere, M. Afzal, Ultrasonic decontamination of prototype fast breeder reactor fuel pins, *Ultrasonics* 54 (2014) 1052–1056, <http://dx.doi.org/10.1016/j.ultras.2013.12.008>.
- [4] K.S. Suslick, D.A. Hammerton, R.E. Cline, The sonochemical hotspot, *J. Am. Chem. Soc.* 108 (1986) 5641–5642.
- [5] E.B. Flint, K.S. Suslick, The temperature of cavitation, *Science* 253 (1991) 1397–1399.
- [6] N.C. Eddingsaas, K.S. Suslick, Evidence for a plasma core during multibubble sonoluminescence in sulfuric acid, *J. Am. Chem. Soc.* 129 (2007) 3838. <Go to ISI>://000245241600032.
- [7] G.J. Price, *Introduction to Sonochemistry*, The Royal Society of Chemistry, Cambridge, 1992.
- [8] T.G. Leighton, From seas to surgeries, from babbling brooks to baby scans: the acoustics of gas bubbles in liquids, *Int. J. Mod. Phys. B* 18 (2004) 3267–3314.
- [9] F.R. Young, *Cavitation*, Imperial College Press, London, 1999.
- [10] T.G. Leighton, *The Acoustic Bubble*, Academic Press, London, 1994.
- [11] P.R. Birkin, D.G. Offen, T.G. Leighton, Experimental and theoretical characterisation of sonochemical cells. Part 2: cell disruptors (ultrasonic horns) and cavity cluster collapse, *Phys. Chem. Chem. Phys.* 7 (2005) 530–537, <http://dx.doi.org/10.1039/b416658b>.
- [12] D.G. Offen, P.R. Birkin, T.G. Leighton, An electrochemical and high-speed imaging study of micropore decontamination by acoustic bubble entrapment, *Phys. Chem. Chem. Phys.* 16 (2014) 4982–4989, <http://dx.doi.org/10.1039/c3cp55088e>.
- [13] M. Keswani, S. Raghavan, P. Deymier, A novel way of detecting transient cavitation near a solid surface during megasonic cleaning using electrochemical impedance spectroscopy, *Microelectron. Eng.* 108 (2013) 11–15, <http://dx.doi.org/10.1016/j.mee.2013.02.097>.
- [14] M. Keswani, S. Raghavan, P. Deymier, Electrochemical investigations of stable cavitation from bubbles generated during reduction of water, *Ultrason. Sonochem.* 21 (2014) 1893–1899, <http://dx.doi.org/10.1016/j.ultsonch.2014.04.009>.
- [15] T.G. Leighton, P. Birkin, D. Offen, A new approach to ultrasonic cleaning, in: *Proc. Int. Congr. Acoust.*; 2013: pp. 075029–075029. <http://dx.doi.org/10.1121/1.4799209>.
- [16] C.J.B. Vian, *A Comparison of Measurement Techniques for Acoustic Cavitation*, University of Southampton, 2007.
- [17] P.R. Birkin, R. O'Connor, C. Rapple, S.S. Martinez, Electrochemical measurement of erosion from individual cavitation events generated from continuous ultrasound, *J. Chem. Soc., Faraday Trans.* 94 (1998) 3365–3371.
- [18] R.G. Compton, J.C. Eklund, F. Marken, T.O. Rebbitt, R.P. Akkermans, D.N. Waller, Dual activation: coupling ultrasound to electrochemistry – an overview, *Electrochim. Acta* 42 (1997) 2919–2927.
- [19] H.H. Zhang, L.A. Coury, Effects of high-intensity ultrasound on glassy-carbon electrodes, *Anal. Chem.* 65 (1993) 1552–1558.
- [20] J.C. Eklund, D.N. Walker, T.O. Rebbitt, F. Marken, R.C. Compton, Organic sonoelectrochemistry. Reduction of fluorescein in the presence of 20 kHz power ultrasound: an EC' reaction; 1995, pp. 198–1984.
- [21] H.N. McMurray, B.P. Wilson, Mechanistic and spatial study of ultrasonically induced luminol chemiluminescence, *J. Phys. Chem. A* 103 (1999) 3955–3962, <http://dx.doi.org/10.1021/jp984503r>.
- [22] M. Hauptmann, S. Brems, H. Struyf, P. Mertens, M. Heyns, S. De Gendt, et al., Time-resolved monitoring of cavitation activity in megasonic cleaning systems, *Rev. Sci. Instrum.* 83 (2012) 034904, <http://dx.doi.org/10.1063/1.3697710>.
- [23] M. Hauptmann, H. Struyf, P. Mertens, M. Heyns, S. De Gendt, C. Glorieux, et al., Towards an understanding and control of cavitation activity in 1 MHz ultrasound fields, *Ultrason. Sonochem.* 20 (2013) 77–88, <http://dx.doi.org/10.1016/j.ultsonch.2012.05.004>.
- [24] M. Hodnett, M.J. Choi, B. Zeqiri, Towards a reference ultrasonic cavitation vessel. Part 1: preliminary investigation of the acoustic field distribution in a 25 kHz cylindrical cell, *Ultrason. Sonochem.* 14 (2007) 29–40, <http://dx.doi.org/10.1016/j.ultsonch.2006.01.003>.
- [25] T.G. Leighton, P.R. Birkin, M. Hodnett, B. Zeqiri, J.F. Power, G.J. Price, et al., Characterisation of measures of reference acoustic cavitation (COMORAC): an experimental feasibility trial, *Sound Vib.* 661 (2005) 37–94.
- [26] M.J. Pickworth, P.P. Dendy, P.R. Twentymann, T.G. Leighton, Studies of the cavitation effects of clinical ultrasound by sonoluminescence: 4. The effect of therapeutic ultrasound on cells in monolayer culture in a standing wave field, *Phys. Med. Biol.* 34 (1989) 1553–1560. <<http://www.ncbi.nlm.nih.gov/pubmed/2587626>>.
- [27] P.R. Birkin, D.G. Offen, P.F. Joseph, T.G. Leighton, Cavitation, shock waves and the invasive nature of sonoelectrochemistry, *J. Phys. Chem. B* 109 (2005) 16997–17005, <http://dx.doi.org/10.1021/jp051619w>.
- [28] University of Southampton, Cleaning apparatus and method, and monitoring thereof. International Patent application PCT/EP2010/062448 filed 26 August

2010. Published 03 March 2011 under WO 2011/023746. Claiming priority from GB 0914836.2.
- [29] P.R. Birkin, Y.E. Watson, T.G. Leighton, K.L. Smith, Electrochemical detection of Faraday waves on the surface of a gas bubble, *Langmuir* 18 (2002) 2135–2140.
- [30] A.R. Williams, D.E. Hughes, W.L. Nyborg, Hemolysis near a transversely oscillating wire, *Science* 169 (1970) 871–873.
- [31] J.A. Rooney, Hemolysis near an ultrasonically pulsating bubble, *Science* 169 (1970) 869–871.
- [32] E. Maisonhaute, C. Prado, P.C. White, R.G. Compton, Surface acoustic cavitation understood via nanosecond electrochemistry. Part III: shear stress in ultrasonic cleaning, *Ultrason. Sonochem.* 9 (2002) 297–303. <<http://www.ncbi.nlm.nih.gov/pubmed/12404794>>.
- [33] J.B. Lonzaga, D.B. Thiessen, P.L. Marston, Uniformly valid solution for acoustic propagation in weakly tapered circular waveguides: liquid jet example, *J. Acoust. Soc. Am.* 124 (2008) 151–160, <http://dx.doi.org/10.1121/1.2932348>.
- [34] J.B. Lonzaga, C.F. Osterhoudt, D.B. Thiessen, P.L. Marston, Liquid jet response to internal modulated ultrasonic radiation pressure and stimulated drop production, *J. Acoust. Soc. Am.* 121 (2007) 3323–3330, <http://dx.doi.org/10.1121/1.2734493>.
- [35] P.R. Birkin, D.G. Offen, C.J.B. Vian, T.G. Leighton, A.O. Maksimov, Investigation of noninertial cavitation produced by an ultrasonic horn, *J. Acoust. Soc. Am.* 130 (2011) 3297–3308, <http://dx.doi.org/10.1121/1.3650537>.
- [36] E. Maisonhaute, P.C. White, R.G. Compton, Surface acoustic cavitation understood by nanosecond electrochemistry, *J. Phys. Chem. B* 105 (2001) 12087–12091.
- [37] E. Maisonhaute, B.A. Brookes, R.G. Compton, Surface acoustic cavitation understood via nanosecond electrochemistry. 2. The motion of acoustic bubbles, *J. Phys. Chem. B* 106 (2002) 3166–3172. <Go to ISI>://000174589000021.
- [38] R. Nabergoj, A. Francescutto, On thresholds for surface waves on resonant bubbles, *J. Phys.* 40 (1979), <http://dx.doi.org/10.1051/jphyscol:1979854>. C8-306–C8-309.
- [39] W.E. Rowe, W.L. Nyborg, Changes in the electrode process brought about by small scale acoustic streaming, *J. Acoust. Soc. Am.* 39 (1966) 965–971.
- [40] W.L. Nyborg, M.I.L. Seegall, Effects of acoustic microstreaming at electrodes, in: L. Cremer (Ed.), *Proc. 3rd Int. Congr. Acoust.*, Elsevier, 1960, pp. 346–348.
- [41] C.C. Church, A method to account for acoustic microstreaming when predicting bubble growth rates produced by rectified diffusion, *J. Acoust. Soc. Am.* 84 (1988) 1758–1764.
- [42] P.R. Birkin, T.G. Leighton, Y.E. Watson, The use of acoustoelectrochemistry to investigate rectified diffusion, *Ultrason. Sonochem.* 11 (2004) 217–221. <Go to ISI>://000221062200020.
- [43] P.R. Birkin, D.G. Offen, C.J.B. Vian, T.G. Leighton, Electrochemical “Bubble Swarm” enhancement of ultrasonic surface cleaning, *Phys. Chem. Chem. Phys.* 17 (2015) 21709–21715.
- [44] P.R. Birkin, S. Silva-Martinez, The effect of ultrasound on mass transfer to a microelectrode, *J. Chem. Soc., Chem. Commun.* (1995) 1807–1808.
- [45] P.R. Birkin, D.G. Offen, T.G. Leighton, A novel dual microelectrode for investigating mass transfer and surface erosion caused by cavitation, *Electrochem. Commun.* 6 (2004) 1174–1179.
- [46] C.R.S. Hagan, L.A. Coury, Comparison of hydrodynamic voltammetry implemented by sonication to a rotating-disk electrode, *Anal. Chem.* 66 (1994) 399–405. <Go to ISI>://A1994MU50800014.
- [47] P.R. Birkin, The use of electrochemistry as a tool to investigate cavitation bubble dynamics, in: B. Pollet (Ed.), *Power Ultrasound Electrochem*, Wiley, Chichester, 2012, pp. 45–78.
- [48] R.P. Howlin, S. Fabbri, D.G. Offen, N. Symonds, K.S. Kiang, R.J. Knee, et al., Removal of dental biofilms with an ultrasonically activated water stream, *J. Dent. Res.* 94 (2015) 1303–1309, <http://dx.doi.org/10.1177/0022034515589284>.
- [49] P.R. Birkin, D.G. Offen, C.J.B. Vian, R.P. Howlin, I. Jonathon, T.J. Secker, et al., Cold water cleaning of brain proteins, biofilm and bone - harnessing an ultrasonically activated stream, *Phys. Chem. Chem. Phys.* 17 (2015) 20574–20579.